Geoscience Letters

RESEARCH LETTER

Open Access

Application of the MELTS program to the fractional crystallization of low-alumina alkaline magma on Jeju Volcanic Island, Korea

Hoang Yen Le[1,3], Cheolwoo Chang[2,3*] and Sung-Hyo Yun[2,3]

Abstract

Jeju Volcanic Island is the largest island in South Korea and is considered a continental shelf intraplate volcanic island. In this study, MELTS, a powerful program for modeling magmatic evolution processes, was applied to simulate the fractional crystallization process of the low-alumina alkaline volcanic rock suite on Jeju Island. MELTS modeling was conducted at many isobaric pressures ranging from 2.0 GPa to 0.1 GPa, different oxygen fugacities (fO_2) from FMQ-3 to FMQ + 3, and different H_2O contents. The results demonstrate that the most suitable fractionation model for the Jeju low-alumina alkaline magma involves a pressure of 0.2 GPa to 0.1 GPa and an oxygen fugacity close to the FMQ buffer. Additionally, an H_2O content of 0.5 wt.% is the most consistent with the evolution trend and mineral composition of the natural rock suite on Jeju Island. Although MELTS possesses several limitations in terms of the stability of calibration, such as spinel overestimation and a lack of experiments on hydrous minerals (which should be improved), MELTS performs well in terms of temperature and pressure prediction and in terms of the assessment of other factors of the fractional crystallization process on Jeju Island. Consequently, to evaluate a magmatic process in a particular region, MELTS should be combined with other analyses and not relied upon independently.

Keywords MELTS modeling, Low-alumina alkaline magma fractional crystallization, Jeju Volcanic Island

Introduction

Jeju Island, the largest island in Korea, is an elliptical island on an intraplate continental shelf (Brenna et al. 2012; Choi et al. 2006; Park 1993a, 1993b; Tatsumi et al. 2005). Jeju Volcanic Island exhibits the characteristics of an oceanic island. For many years, the petrology, geochemistry, geomorphology, and other characteristics of Jeju Volcanic Island have been studied comprehensively. The MELTS program has been developed to simulate magmatic evolution processes on the basis of bulk composition (Ghiorso and Sack 1995; Asimow and Ghiorso 1998); hence, it can predict the direction of evolution paths. In this program, each thermodynamic factor, such as temperature, pressure, and oxygen fugacity, can affect the modeling. Consequently, to better understand the formation conditions of Jeju Island, we carried out various calculations and selected the conditions that best match the natural evolution paths.

Fractional crystallization is a significant process affecting magmas on Jeju Island (Tatsumi et al. 2005). Indeed, according to the research of Brenna et al. (2010), the fractionation of clinopyroxene + olivine ± spinel in alkaline magma occurred at approximately 2.0–1.5 GPa beneath Jeju Volcanic Island. In this study, the MELTS program is used to verify the

*Correspondence:
Cheolwoo Chang
iori@pusan.ac.kr
[1] Department of Earth Sciences, Graduate School, Pusan National University, Busan 46241, Republic of Korea
[2] Department of Earth Science Education, Pusan National University, Busan 46241, Republic of Korea
[3] Volcano Specialized Research Center (VSRC), Pusan National University, Busan 46241, Republic of Korea

pressure condition on the basis of thermodynamic principles. Additionally, MELTS can model whole-magma fractionation, not only the pressure conditions, but also other factors, such as temperature, mineral and chemical compositions, and even oxygen fugacity. Currently, MELTS has not been applied to any region in Korea. Consequently, this research will serve as a comparison and reference for subsequent studies.

Regional geology and tectonic setting

Jeju Volcanic Island is an intraplate continental shelf island with an elliptical shape (Brenna et al. 2012; Choi et al. 2006; Park 1993a, 1993b; Tatsumi et al. 2005) located approximately 90 km from the southern coast of the Korean Peninsula (Fig. 1a). This island is 74 km × 32 km in size, with the long axis and short axis oriented in the northeast–southwest and northwest–southeast directions, respectively (Koh et al. 2003) (Fig. 1c). There is contrasting topography in the northern,

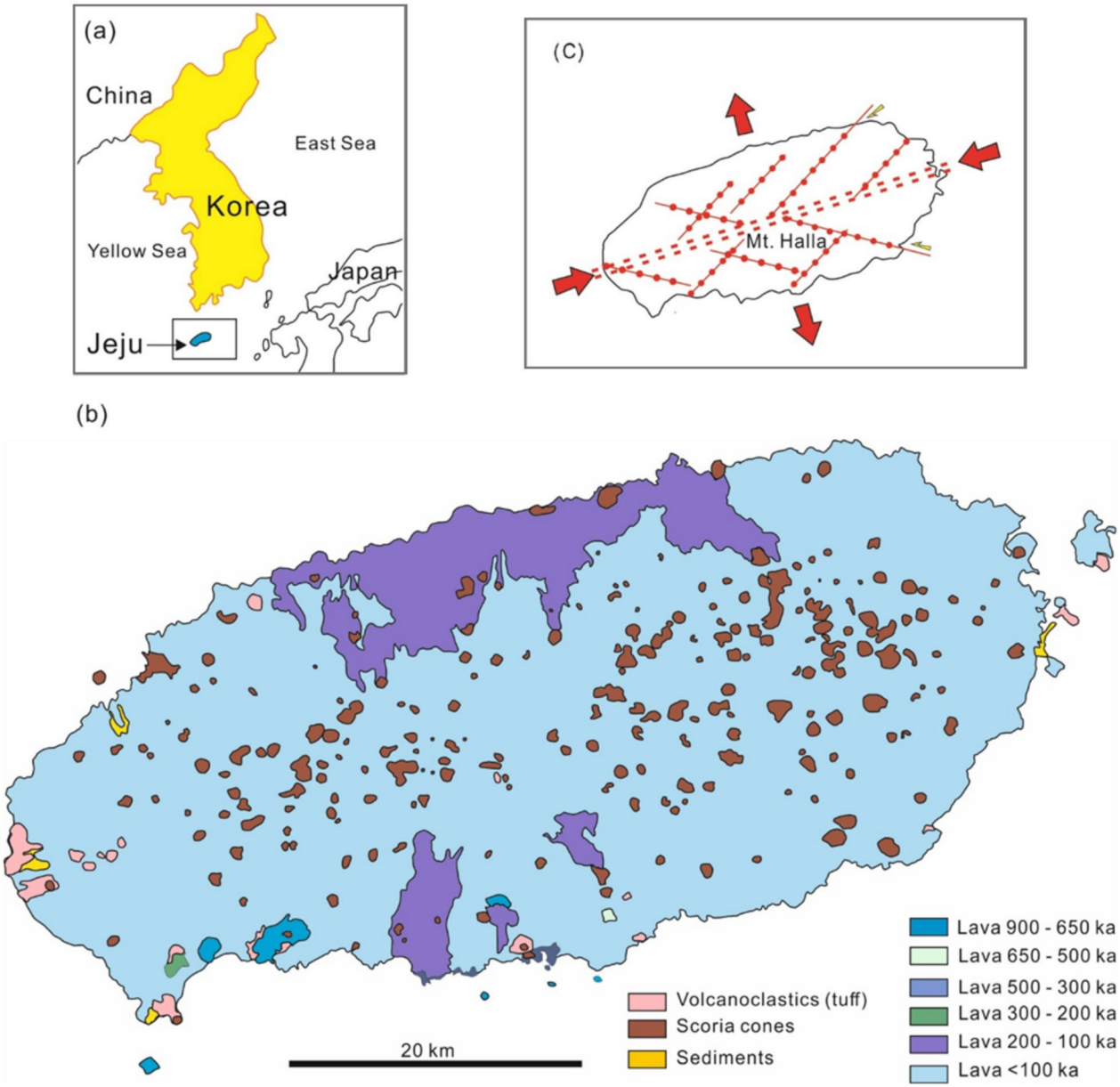

Fig. 1 Location (**a**), surface lava distribution map according to 40Ar—39Ar plateau age (**b**), and expected fracture system (**c**) of Jeju Volcanic Island. Modified after Lee 1982 (**a**); Koh et al. 2013 (**b**); Koh et al. 2003 (**c**)

western and eastern areas of Jeju Volcanic Island; the relief generally slopes gently down to the sea (the same direction as the lava flows), whereas 10-m cliffs dominate the southern coastline, forming waterfalls along this coast on Jeju Volcanic Island. The surface distribution map (Fig. 1b) depicts the dominance of lava flows on the surface, which are no older than 100,000 years BP. Jeju Volcanic Island is dominated by lava flows, with minor phreatomagmatic tuff rings, tuff cones, and sediments. Lee (1982) divided the stratigraphic system into four stages: the basal basalt stage (below sea level), the lava plateau stage, the lava shield (Halla shield volcano) stage, and the scoria cone stage. The basement contains Jurassic to Cretaceous granitoids and unconsolidated sediments, volcaniclastics and pre-Cambrian gneisses, which appear as xenoliths in tuffs and in drill cores (Baek et al., 2014; Choi et al. 2006; Lee 1982; Tatsumi et al. 2005). Spinel peridotite and pyroxenite xenoliths are common in alkali basalt lavas and tuffs and represent mantle-derived components (Yun et al. 1998; Choi et al. 2005; Kil et al. 2008; Brenna et al. 2012).

In terms of alumina content, volcanic rocks on Jeju Volcanic Island are categorized into 3 main series: high-alumina alkaline, low-alumina alkaline and subalkaline rock types corresponding to low, moderate, and high degrees of partial melting, respectively (Tatsumi et al. 2005). In addition, these volcanic rocks have been classified as transitional basaltic suites (Koh 2005) occurring solely in the deep part of eastern Jeju (Brenna 2012).

The contents of P_2O_5 and K_2O and the trace element contents of the lava suites suggest that large-volume lavas on Jeju Volcanic Island are not derived from truly primary sources; instead, these lavas are derived from a homogeneous mantle source and involved melting at several levels and dissimilar depths (Park 1993a, 1993b). According to geochemical and mineralogical characteristics (Tatsumi et al. 2005), a mantle plume was present underneath Jeju Volcanic Island. In their model (Fig. 2), the magma rose from the asthenosphere and reached the highest part of the mantle located under the metasomatized zone, enriching the isotopic components. The partial melting levels are categorized as follows: the lowest level of partial melting generated a high-alumina alkaline magma from an amphibole source with high Al and Sr contents in the lower part of the upper mantle.

Methods

As mentioned previously, there are three main magmatic suites on Jeju Volcanic Island; however, the low-alumina alkaline magma has been interpreted as the suite that possesses the greatest source depth and is less metasomatized than the others (Tatsumi et al. 2005). Consequently, this study focuses on the low-alumina alkaline rock suite. Since many surveys on petrology and geochemistry have been conducted over Jeju Volcanic Island, all of the natural data utilized in this research were collected from published studies. The reference samples were selected from the low-alumina alkaline series in Tatsumi et al. (2005) and trachyte samples around the Paekrogdam (Baengnokdam) summit in Koh et al. (2003) to describe the whole low-alumina alkaline suite on Jeju Volcanic Island. There samples are shown plotted in the TAS classification diagram (Le Bas et al. 1986) (Table 1, Fig. 3). Preferably, the most primitive mafic composition is the best beginning for fractionation simulation. Consequently, in a rock suite, the sample with the lowest SiO_2 content and highest MgO content is the most suitable for MELTS. Therefore, sample CJ10 in the study of Tatsumi et al. (2005), with 47.14 wt.% SiO_2 and 9.85 wt.% MgO, satisfies the starting composition for modeling the magma evolution process via MELTS in this study. This sample is also considered the inferred primary magma composition for the low-alumina alkaline suite in Tatsumi et al. (2005).

In silicate melts, the oxidation state of iron is a significant factor for understanding magma evolution processes both physically and chemically (Osborn 1959; Carmichael and Ghiorso 1990). The ferric–ferrous proportion plays a vital role in melt properties, such as viscosity and density (Lange and Carmichael 1990; Dingwell 1991; Dingwell and Brearley 1988). Moreover, it drives the occurrence of iron-bearing oxides and ferromagnesian silicates, as well as the chemical properties of concurrent melts (Gaillard et al. 2001). For the Jeju Volcanic Island samples, oxygen fugacity is represented relative to the equilibrium of fayalite, magnetite, and quartz (the FMQ buffer); positive values are more oxidizing, whereas negative values are more reducing, and upper mantle oxygen fugacity is thought to be close to the QFM buffer ranging from FMQ^{-4} to FMQ^{+2} (McCammon 2005), as shown in Fig. 4. Moreover, the samples from Jeju Volcanic Island can be classified as oceanic island basalt (OIB), which is typically generated from a mantle plume (Tatsumi et al., 2005), and the oxygen fugacity of mantle plume-related OIB tends to be limited to FMQ to FMQ^{+2} (Ballhaus et al. 1990). Nevertheless, to examine the FMQ conditions more consistently, we performed various calculations from FMQ^{-3} to FMQ^{+3}.

By using pMELTS (Ghiorso et al. 2002) and rhyolite-MELTS (version 1.0.2 and 1.2.0) as alternative versions of MELTS after the study of Gualda et al. (2012), we conducted various calculations of fractional crystallization under various isobaric pressure conditions, from 2.0 to 0.1 GPa (20,000 to 1000 bars), and FMQ levels, from FMQ^{-3} to FMQ^{+3}, to verify previous findings. After these calculations, we compared the results of the two MELTS programs above and compared the results with

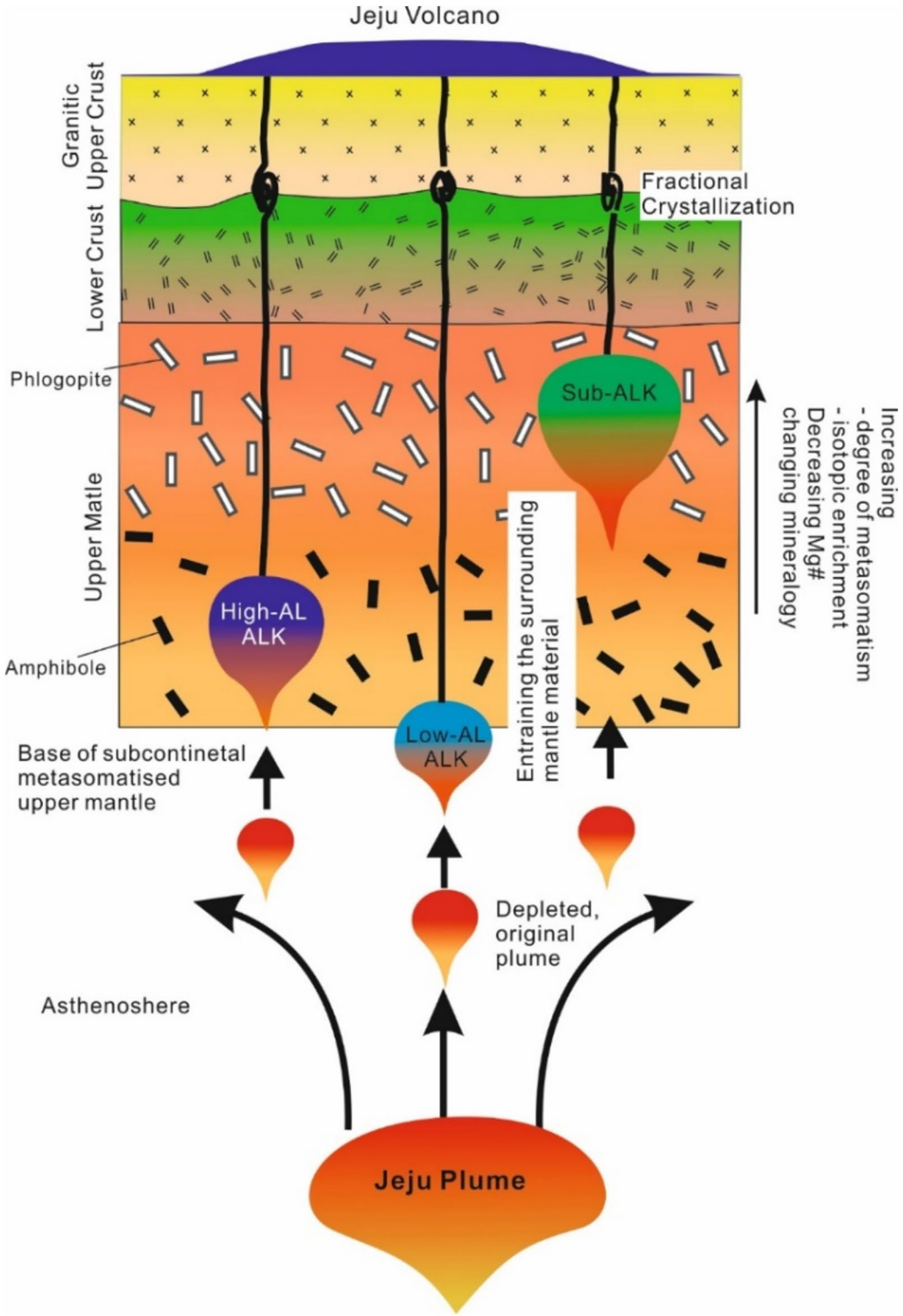

Fig. 2 Modeling of the upper mantle beneath Jeju Volcanic Island (edited after Tatsumi et al. 2005)

published natural samples from other studies to evaluate the accuracy of the calculations. We carried out assessments and comparisons of both the evolution paths and the mineral components in the natural rock suite on Jeju Volcanic Island.

pMELTS is suitable for modeling at pressures above 1.0 GPa, whereas rhyolite-MELTS is suitable for

Table 1 Bulk compositions of natural samples collected from Jeju Volcanic Island were compared with those obtained via MELTS modeling

Sample	CJ05	CJ06	CJ09	CJ10	CJ11	CJ12	CJ13	CJ16	CJ17
SiO_2	50.98	48.95	49.46	47.14	48.55	47.87	55.55	48.86	49.53
TiO_2	2.22	3.18	3.03	2.39	2.92	3.14	1.53	2.58	2.54
Al_2O_3	16.4	16.63	16.56	13.84	16.51	16.25	16.88	16.04	16.47
Fe_2O_3	11.89	13.41	12.76	12.42	12.71	13.48	10.39	12.19	11.9
FeO									
MnO	0.16	0.15	0.16	0.16	0.15	0.15	0.16	0.15	0.15
MgO	4.71	3.95	3.89	9.85	5.35	5.42	2.09	6.04	5.27
CaO	6.94	7.75	7.27	9.55	8.41	8.3	4.9	7.96	7.56
Na_2O	4.28	3.89	4.11	2.81	3.69	3.65	5.10	3.62	4.12
K_2O	2.13	1.43	1.93	1.36	1.22	1.33	2.84	1.91	2.00
P_2O_5	0.76	0.63	0.74	0.43	0.57	0.56	0.81	0.68	0.69
Total	100.47	99.97	99.91	99.95	100.08	100.15	100.25	100.03	100.23
Sample	**CJ18.1**	**CJ18.2**	**CJ19**	**CJ23**	**CJ24**	**CJ26.2**	**CJ28**	**CJ29**	**CJ30.1**
SiO_2	49.11	48.85	50.12	53.76	49.06	48.63	49.3	48.67	59.02
TiO_2	2.96	2.99	2.54	1.77	2.64	2.64	2.44	2.71	1.00
Al_2O_3	16.16	16.06	16.47	16.9	15.47	15.63	15.25	16.61	17.41
Fe_2O_3	12.84	12.88	11.51	11.31	12.8	12.22	12.08	12.38	7.97
FeO									
MnO	0.16	0.16	0.15	0.17	0.15	0.15	0.15	0.14	0.13
MgO	4.8	4.67	4.83	2.6	6.28	6.79	7.63	5.85	1.02
CaO	7.71	7.75	8.63	5.58	8.48	7.87	8.5	9.25	3.15
Na2O	3.85	3.94	3.83	4.85	3.54	3.65	3.37	3.35	5.65
K2O	1.75	1.74	1.71	2.46	1.21	1.88	1.44	0.91	3.70
P_2O_5	0.89	0.89	0.56	0.84	0.51	0.60	0.49	0.46	0.33
Total	100.23	99.93	100.35	100.24	100.14	100.06	100.65	100.33	99.38
Sample	**CJ30.2**	**CJ31**	**CJ32**	**CJ33**	**CJ34**	**CJ36**	**CJ38**	**CJ40**	**H1**
SiO_2	49.93	49.86	49.95	48.24	48.4	49.63	48.86	49.58	65.15
TiO_2	2.56	2.58	2.45	2.74	2.13	2.42	2.65	2.42	0.29
Al_2O_3	16.45	16.55	15.93	15.6	14.55	15.61	16.3	15.58	16.75
Fe_2O_3	12.08	11.71	11.85	12.86	11.99	11.61	12.35	11.61	2.41
FeO									2.16
MnO	0.15	0.15	0.15	0.15	0.16	0.14	0.15	0.14	0.14
MgO	5.42	4.56	6.01	6.61	9.14	6.69	5.21	6.7	0.25
CaO	8.00	8.41	7.55	7.83	9.35	8.15	7.63	8.16	1.09
Na_2O	3.85	3.88	3.88	2.82	3.08	3.72	3.92	3.62	5.66
K_2O	1.50	1.77	1.97	1.43	1.16	1.60	1.85	1.57	5.62
P_2O_5	0.56	0.58	0.61	0.51	0.4	0.52	0.64	0.54	0.05
Total	100.5	100.05	100.35	98.79	100.36	100.09	99.56	99.92	99.57
Sample	**H2**	**H3**	**H4**	**H5**	**H6**	**H8**	**H9**	**H10**	**H12**
SiO_2	64.86	63.2	50.87	53.1	64.04	53.71	65.17	49.44	51.97
TiO_2	0.31	0.45	2.40	1.84	0.28	1.73	0.27	2.51	2.23
Al_2O_3	16.39	16.76	15.88	17.86	16.23	17.93	16.5	15.78	16.50
Fe_2O_3	2.63	3.00	3.49	3.33	2.37	3.22	2.35	3.26	3.8
FeO	2.37	2.70	7.33	5.56	2.13	5.39	2.12	7.61	6.35
MnO	0.16	0.17	0.19	0.17	0.14	0.17	0.14	0.2	0.19
MgO	0.30	0.48	4.61	2.76	0.25	2.63	0.25	5.62	3.33
CaO	1.38	1.90	7.77	6.77	1.15	6.56	1.25	8.01	7.04
Na_2O	5.63	5.58	3.80	4.47	5.57	4.40	5.57	3.48	4.14
K_2O	5.50	5.19	2.10	2.55	5.53	2.65	5.56	1.84	2.43
P_2O_5	0.06	0.12	0.60	0.62	0.05	0.59	0.05	0.65	0.69
Total	99.59	99.55	99.04	99.03	97.74	98.98	99.23	98.40	98.67

Table 1 (continued)

Data from Tatsumi et al. 2005 (CJ05 to CJ40) and Koh et al. 2003 (H1 to H12)

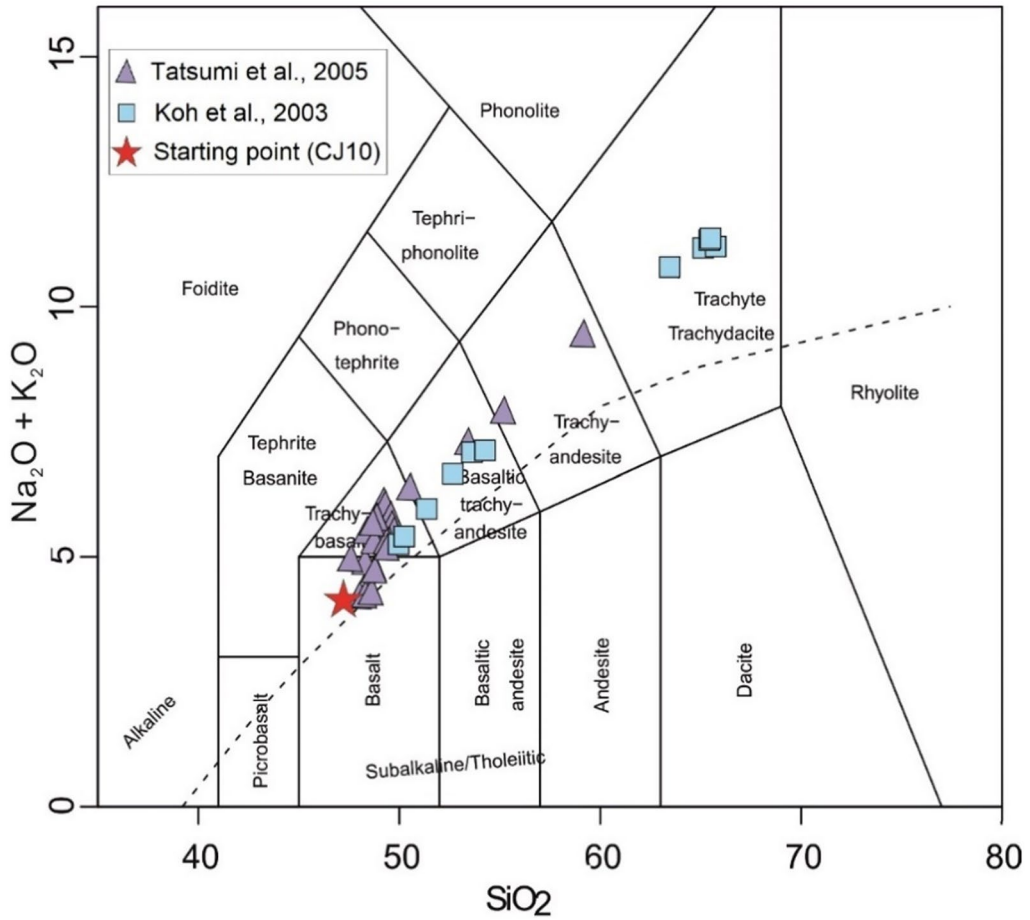

Fig. 3 Published natural samples from Jeju Volcanic Island from studies by Tatsumi et al. (2005) and Koh et al. (2003) plotted in a TAS diagram (after Le Bas et al. 1986)

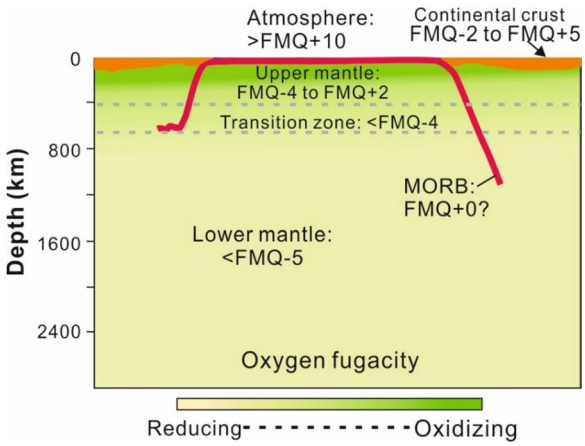

Fig. 4 The change in oxygen fugacity corresponds to the depth beneath the Earth's crust (edited after McCammon 2005)

modeling at pressures less than 1.0 GPa. Consequently, two separate MELTS programs are used in this study: pMELTS handles modeling for pressures ranging from 2.0 to 1.0 GPa, and rhyolite-MELTS handles modeling for pressures ranging from 1.0 to 0.1 GPa. At each pressure level, various log units of oxygen fugacity, FMQ^{-3} to FMQ^{+3}, were used. In this part, the calculations are divided into three groups on the basis of pressure: the first group comprises the results from the pMELTS program; in the second group, pressures from 1.0 to 0.4 GPa are simulated by the rhyolite-MELTS; and the last group includes the remaining pressure levels, 0.2 GPa and 0.1 GPa. However, more tests were performed when water was added to the calculations; hence, the rhyolite-MELTS versions 1.0.2 and 1.2.0 were applied

to for modeling of anhydrous and hydrous systems, respectively.

Results and discussion

As demonstrated in Fig. 5, the evolution paths from FMQ^{+1} to FMQ^{-3} tend to curve toward the left side of the diagram, especially at high-pressure levels, whereas those from FMQ^{+2} and FMQ^{+3} display slightly curved lines and plot along the sample suite. At 2.0 GPa and 1.8 GPa, the modeling results of FMQ^{+3} match those of the Jeju rock suite; however, the modeling results at 1.8 GPa fail since they accounts for only half of the sample suite. In the next level, from 1.6 to 1.4 GPa, the natural sample line is distributed between FMQ^{+2} and FMQ^{+3}; it is closer to FMQ^{+3} at 1.6 GPa and almost coincides with FMQ^{+2} at 1.4 GPa. FMQ^{+2} seemingly fits the Jeju sample line well at 1.2 and 1.0 GPa, but mismatches occur at the ends of the lines. Nevertheless, none of the FMQ^{+2} and FMQ^{+3} modeling paths from 2.0 to 1.0 GPa simulated by pMELTS plot along the natural sample suite line.

The second group, i.e., < 1.0 GPa, illustrates that the use of rhyolite-MELTS is more reasonable than the use of pMELTS, and the differences between the 2.0–1.0 GPa and 1.0–0.4 GPa modeling paths in the TAS diagram are distinct (Fig. 6). The angle between the horizontal axis and the evolution paths simulated by rhyolite-MELTS decreases gradually from nearly vertical to approximately 45°, especially the group with oxygen fugacities from FMQ^{-3} to FMQ^{+2}. On the other hand, FMQ^{+3} does not change much and is always close to the Jeju alkaline suite. At 1.0 GPa, the modeling line plots along the sample suite but does not overlap entirely; overlap occurs at pressures ranging between 0.8 and 0.6 GPa. However, the first part of the modeling line at 0.4 GPa is rather separated from the sample points. In addition to the difference in trends, the simulated lines at the FMQ^{+3} buffer have dissimilar lengths and tend to maintain a longer line of coincidence with a drop in pressure.

The final group, at 0.2 and 0.1 GPa, was subjected to two separate conditions, one in which the original composition is the same as that of the other runs and a second in which 0.5 wt.% H_2O is added to the starting member (Fig. 7). At first glance, the most obvious difference between the two is the length of the modeling lines, which are longer for the second model than the real evolution paths. The occurrence of water in the system not only extends modeling paths but also tilts down all 7 oxygen fugacities. At 0.2 GPa, the modeled line overlaps the natural suite at FMQ^{+2} for the anhydrous starting member and at FMQ for the 0.5 wt.% H_2O starting member. Furthermore, these lines coincide with each other at 0.1 GPa. The Jeju alkaline suite is well modeled by FMQ^{+1} with 0 wt.% H_2O, but at the match is still good at the FMQ buffer when the system contains a small proportion of H_2O. Although the modeling line also curves down at the end of the path, as in other calculations, no published data are available for this section. Consequently, it is important for future studies to explore the entire rock suite on Jeju Volcanic Island to verify the MELTS modeling.

On the basis of the comparison of modeled evolution paths and the natural Jeju alkaline rocks in the TAS diagram in the previous section, paths that coincide with real sample points are selected to simulate crystallization paths. The calculations of the model with the FMQ^{+3} buffer match the suite at most pressure levels from 2.0 to 1.0 GPa in pMELTS and from 1.0 to 0.4 GPa in rhyolite-MELTS. Afterward, the matched oxygen fugacities start to decrease gradually from 0.2 GPa. The mineral compositions also differ among the different pressure levels.

The results from pMELTS demonstrate that, above 2.0 GPa, clinopyroxene and spinel are two of the first minerals to crystallize, followed by orthopyroxene, which is not present at 1.8 GPa. The first crystallizations occur at approximately 1,460 °C, 1410 °C and 1,380 °C; however, these temperatures decrease proportionally with pressure. Feldspars begin to crystallize at approximately 1,200 °C at 1.6 GPa. On the other hand, olivine is absent in all of the models from 2.0 to 1.4 GPa and starts to occur in the model at ≤ 1.2 GPa at approximately 1150 °C. Curiously, most of the minerals crystallize in one phase, except spinel, the crystallization of which is divided into 2 separate phases at 2.0 GPa. The first occurs briefly from 1,410 to 1,390 °C, and the second occurs from approximately 1,330 °C to 1,190 °C (Fig. 8). The mineral phases that formed during the fractional crystallization process of the Jeju low-alumina alkaline magma include olivine, clinopyroxene, plagioclase and magnetite (Tatsumi et al., 2005). Hence, the absence of olivine from 2.0 GPa to 1.4 GPa is incompatible with the mineral assemblage of the Jeju alkaline rocks. The results seem more feasible when olivine starts to join the system at 1.2 GPa; however, the presence of orthopyroxene leads to a contradiction once again.

In the second group, olivine is still absent from 1.0 GPa to 0.4 GPa in the rhyolite-MELTS operation.

(See figure on next page.)

Fig. 5 Comparison of evolution paths between the pMELTS model (dashed line) and natural samples (point) from 2.0 to 1.0 GPa under various oxygen fugacities on the TAS diagram (after Le Bas et al. 1986)

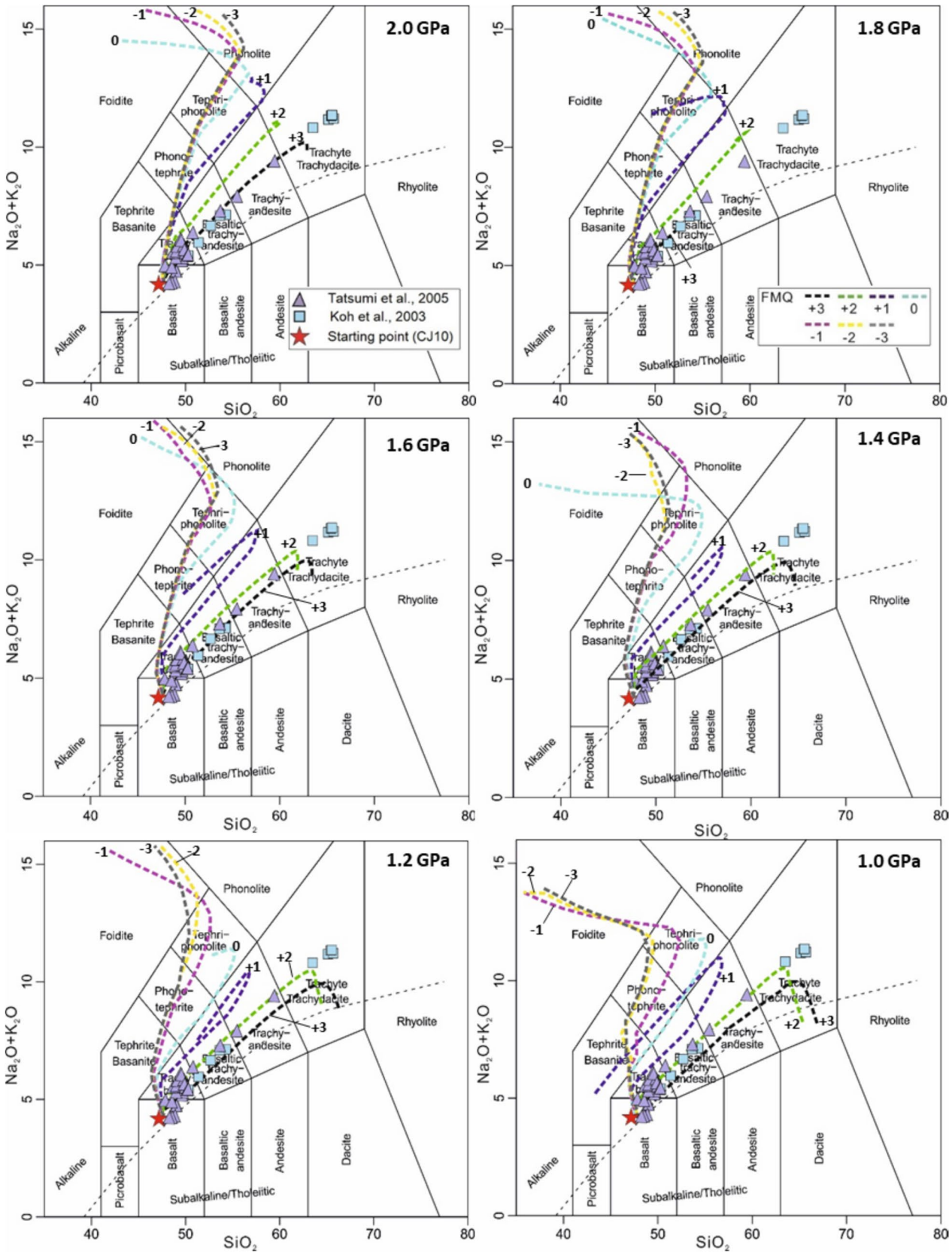

Fig. 5 (See legend on previous page.)

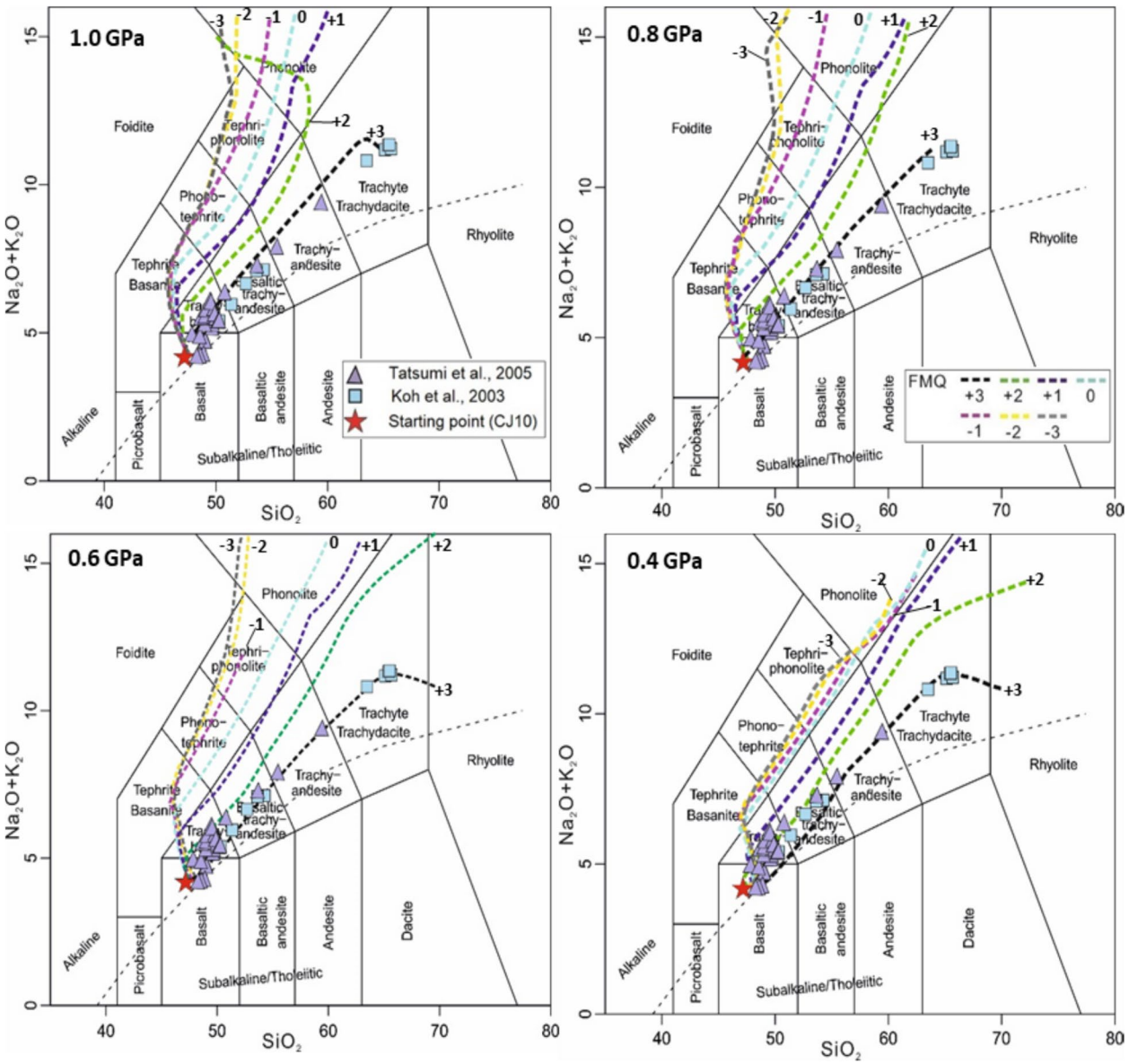

Fig. 6 Comparison of the evolution paths between the rhyolite-MELTS model and the natural samples from 1.0 to 0.4 GPa at various oxygen fugacities on the TAS diagram (after Le Bas et al. 1986)

Nevertheless, at 1.0 GPa or less, other new minerals, such as rhm-oxide and whitlockite, form in the magmatic system. The decrease in the crystallization temperature range is proportional to the decrease in pressure; for example, at 1.0 GPa, magma experiences a fractional crystallization process from approximately 1,400 °C to 1,100 °C, whereas at 0.4 GPa, this range begins at approximately 1300 °C and ends at 1000 °C. In this pressure interval, spinel continues to form during one phase near the beginning of the whole crystallization process. In addition, orthopyroxene and clinopyroxene also stably crystallize in one continuous phase. Olivine is still absent in this second group. In particular, rhm-oxide joins the system intermediately after the spinel crystallization phase ends. In the MELTS program, the spinel phase is equal to the spinel and magnetite phases in natural rocks, and when rhm-oxide is present, ilmenite is present. Whitlockite is an odd component because of its representative rock mineral composition; however, it is dominant in most runs of rhyolite-MELTS at pressures below 1.0 GPa. The presence of whitlockite supplies an anhydrous calcium phosphate phase; in nature, the components are

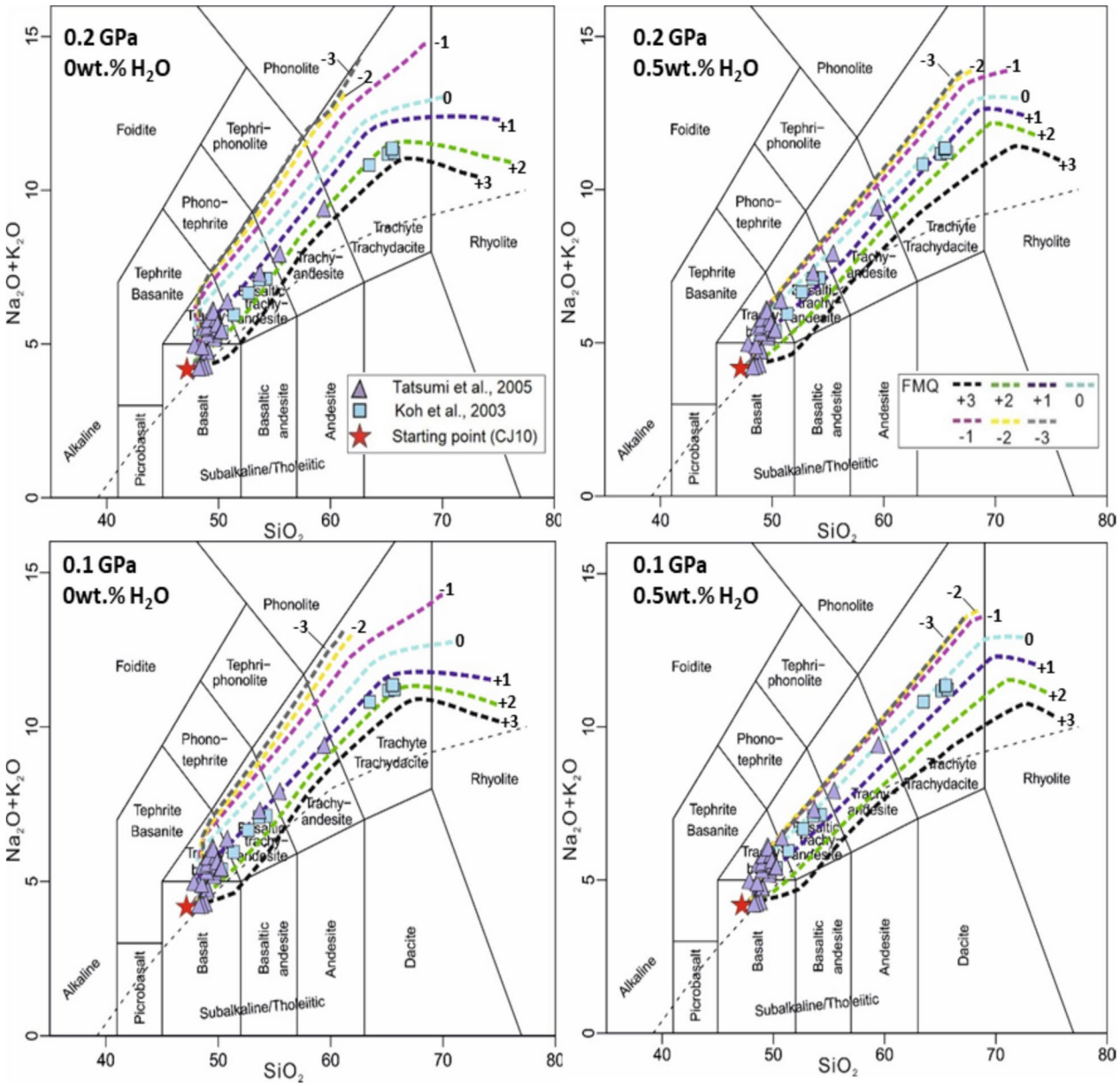

Fig. 7 Comparison of the evolution paths between the rhyolite-MELTS model samples and the natural samples from 0.2 to 0.1 GPa under different oxygen fugacities and H_2O contents (after Le Bas et al. 1986)

not completely dry, and the accessory mineral is apatite. Consequently, whitlockite should be considered apatite (Fig. 9). In summary, despite the presence of new mineral phases, such as whitlockite and rhm-oxide, which correspond to apatite and ilmenite mineral compositions in the natural Jeju alkaline rock, the occurrence of orthopyroxene and lack of olivine phases during modeling indicate that there is no obvious pressure window for Jeju alkaline fractional crystallization.

The calculations in the last group were performed under two conditions with two different H_2O contents and the same oxygen fugacity regimes. The results demonstrate that the evolution paths in the TAS diagram tilt down when the system possesses a small amount of H_2O. Consequently, in this group, each pressure is modeled in 2 separate calculations with 0 wt.% H_2O and 0.5 wt.% H_2O. In the case of absolutely anhydrous magma, the same bulk compositions and oxygen fugacities as those in the previous runs, as well as the mineral

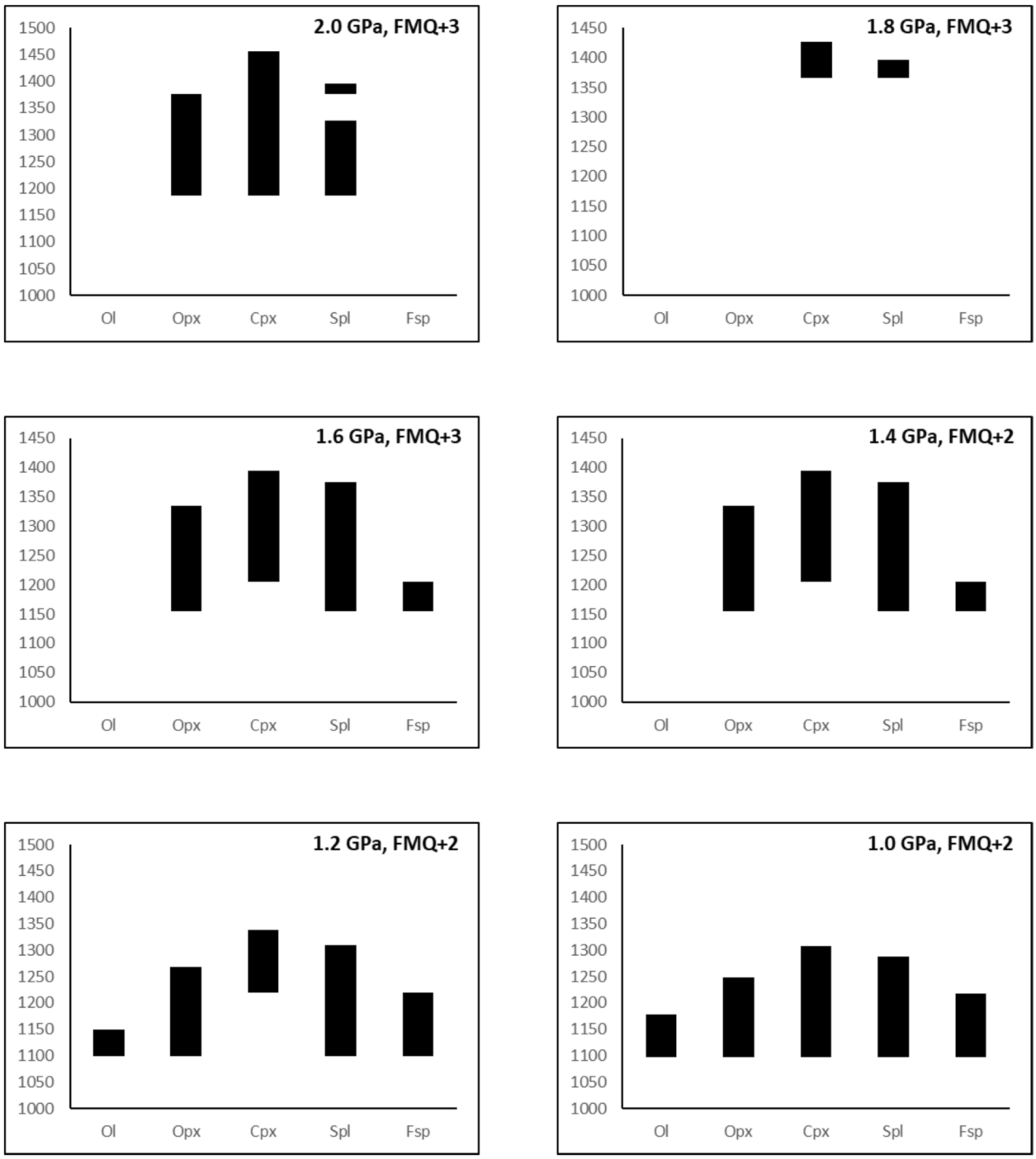

Fig. 8 Crystallization paths of CJ01 at pressures ranging from 2.0 GPa to 1.0 GPa, as simulated by the pMELTS program

compositions as those in the previous calculation above 0.2 GPa, were used. At 0.2 GPa, olivine starts to occur during modeling. Olivine occurs at approximately 1,250–1,200 °C at 0.2 GPa with the FMQ^{+2} buffer and at 1,260–1,100 °C at 0.1 GPa with the FMQ^{+1} buffer. However, orthopyroxene still exists during the simulation processes. The presence of H_2O enhances the similarity between the modeling results and the Jeju low-alumina alkaline magma. In the hydrous system, at both 0.2 and 0.1 GPa under the same FMQ buffer, the mineral phase compositions include olivine, clinopyroxene, spinel, feldspar, apatite, and rhm-oxide, which are also present

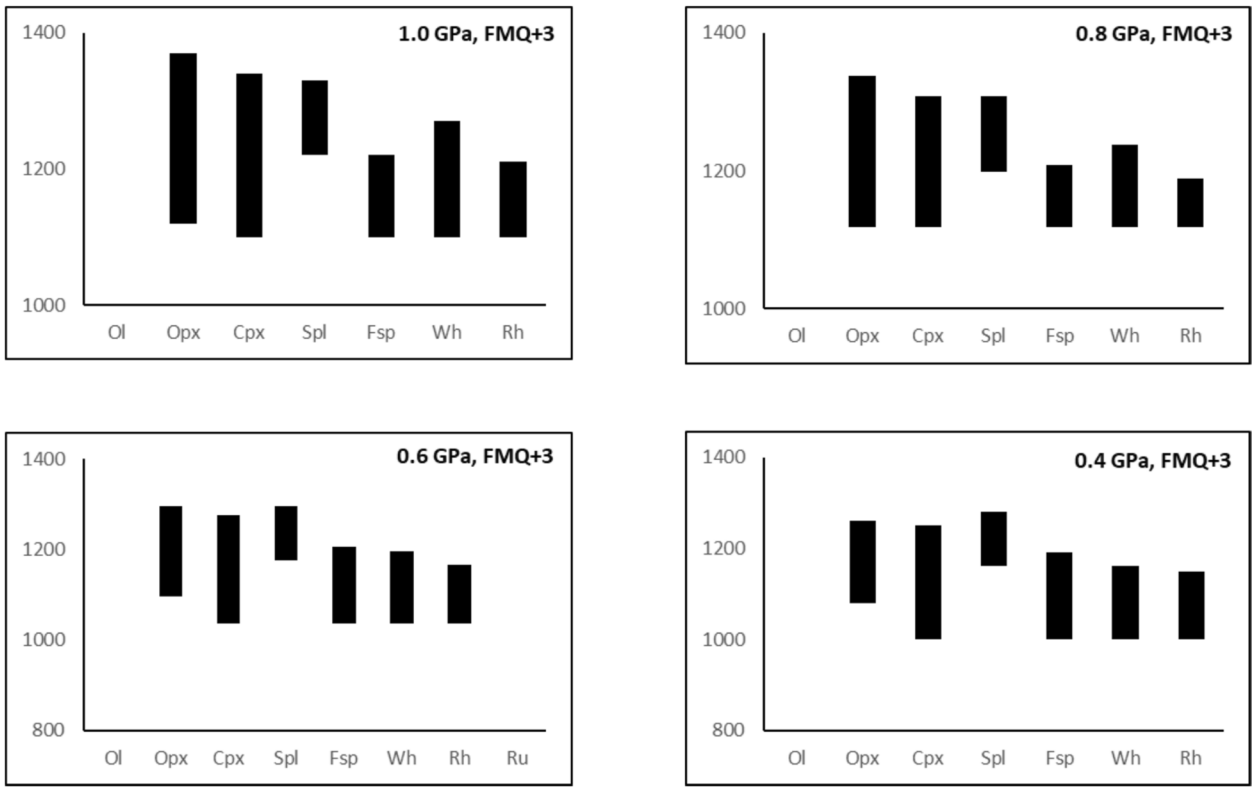

Fig. 9 Crystallization paths of CJ01 at pressures ranging from 1.0 GPa to 0.4 GPa, as simulated by the rhyolite-MELTS program

in the natural alkaline rocks on Jeju Volcanic Island. However, the spinel phases are still likely to be overestimated in all calculations, which is a defect of the MELTS algorithm (Fig. 10).

The evolution paths between 0.2 GPa and 0.1 GPa are rather similar to each other (Fig. 11). While most correlation diagrams exhibit consistency between the evolution paths of the MELTS modeling and those of the natural Jeju suite, some of them exhibit dissimilarity, despite rhyolite-MELTS having been proven to be an extremely powerful program for magmatic evolution modeling. The variation chart illustrates the correspondence between MgO and Al_2O_3, and the evolution lines of rhyolite-MELTS are bent down and separated from the natural suite when spinel starts to crystallize in the modeling system. Although spinel participated in the fractional crystallization process beneath Jeju Volcanic Island together with olivine and clinopyroxene, the modeling overestimates the degree of spinel crystallization by not halting the crystallization process at the appropriate time, as exhibited by the successive decrease in Al_2O_3. Spinel overestimation in rhyolite-MELTS is still an unresolved issue, as mentioned in the previous section. In addition, apatite is another unstable mineral phase in this calculation, as demonstrated via the correlation between MgO and P_2O_5. Indeed, although the apatite modeling evolution paths also decrease, they continue to generate paths higher than those of the real sample suite, where they should be curved instead. This deviation may be due to simulation failures for hydrous minerals, such as with amphibole and biotite, which is a prominent limitation for hydrous modeling by rhyolite-MELTS (Gualda et al. 2012). The last inconsistency between rhyolite-MELTS modeling and the real data corresponds to MgO and CaO. While the contents of these oxides gradually decrease in the Jeju alkaline suite during magma ascent, the rhyolite-MELTS lines increase at the beginning and then dip down until clinopyroxene forms in the magmatic system. Consequently, the clinopyroxene produced by MELTS crystallized later than that in the natural rocks. Indeed, MELTS developers have been attempting to increase the stability of spinel and to perform more experiments on hydrous mineral phases. Overall, although MELTS accurately simulates the fractional crystallization process on Jeju Volcanic Island, it needs to be combined with more experiments and analyses and should not be relied upon independently.

A successful model must match the data trend in every oxide and every evolution diagram simultaneously. A failure to match in any presentation is a failure of the model.

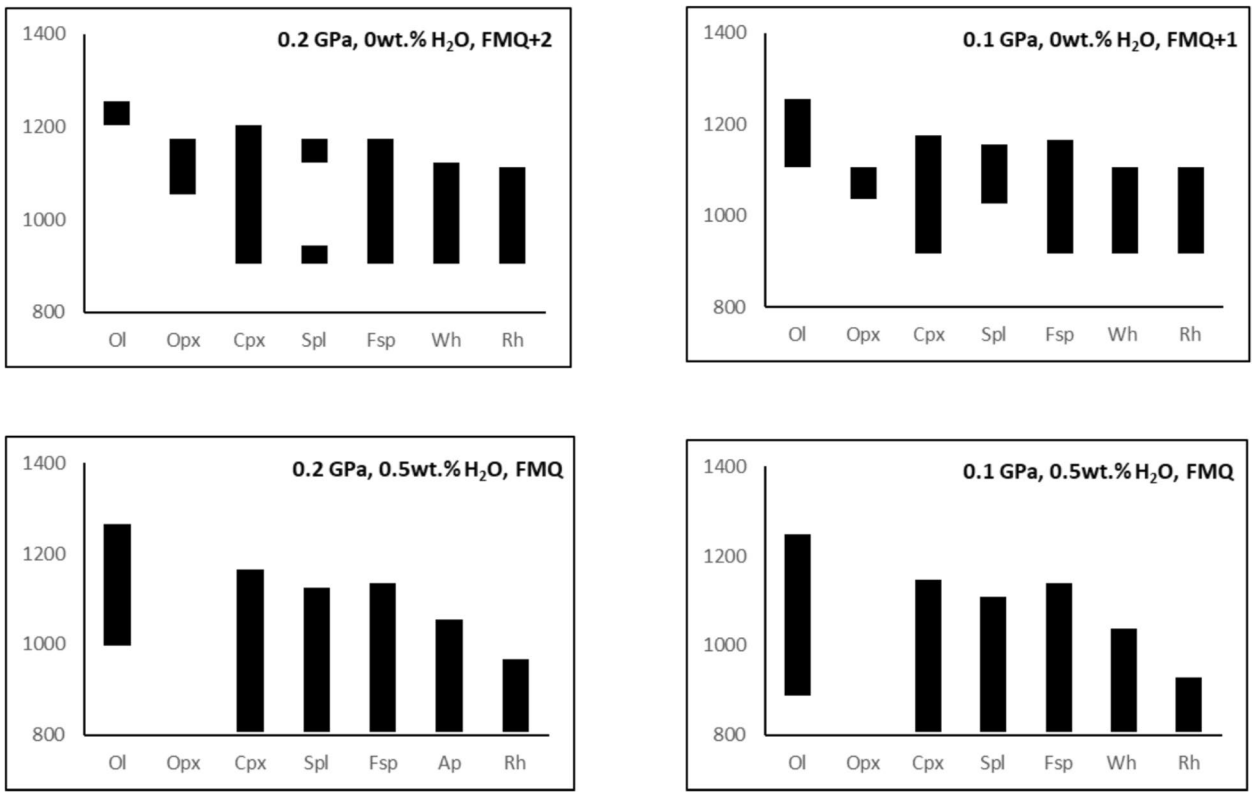

Fig. 10 Crystallization paths of CJ01 at pressures ranging from 0.2 GPa to 0.1 GPa simulated by the rhyolite-MELTS program

Hence for quickly presenting the results of a broad survey of parameters, any diagram can be used to rule out failed models and narrow the range of parameters to the subset of models that deserve further scrutiny. In this case, the TAS diagrams allow us to quickly see that the pMELTS models at high pressure will not work, and to select a subset of low pressure models with either high fO2 or some water content. Then those small number of models that appear to work in the TAS diagram can be examined in the full set of Harker diagrams. For clarity, only a small number of successful models are shown. It would simply complicate the diagrams to plot model runs that have already failed to match on the TAS diagram. However, we would show the difference in one or more of the Harker diagrams between models like (rMELTS, 0.6 GPa, QFM + 3, 0 H2O) and (rMELTS, 0.1 GPa, QFM + 0, 0.5% H_2O). These both appear to work perfectly in TAS plots. We know that only one of these will look good in Harker diagrams, but the paper does not show this. So, we will continue in our next study to add a small number of the models that give the very best fit in TAS to enough of the Harker diagrams to show why they were rejected.

By looking at how the Harker diagram trends change slope when phases appear or disappear on the liquidus, we can add some useful discussion text that points out how the stability of each phase depends on variables like P, fO2, H_2O and therefore give some guidance as to why the best model is the best model.

Finally, some comment on the CaO vs. MgO Harker plot (Fig. 11) is needed. In many of the Harker diagrams, it is impossible to distinguish between the liquid line of descent itself and mixing lines obtained by recharging an evolved magma along the liquid line of descent with some of the starting liquid. But these can be distinguished in CaO vs. MgO. I think the Tatsumi et al. (2005) data showing decreasing CaO early in the evolution trend are hard to explain unless cpx is on the liquidus, unless you consider that these may

(See figure on next page.)

Fig. 11 The variation diagrams revealing the crystallization paths of rhyolite-MELTS at 0.2 GPa and 0.1 GPa compared with those of the natural alkaline rock suite at Jeju Volcanic Island

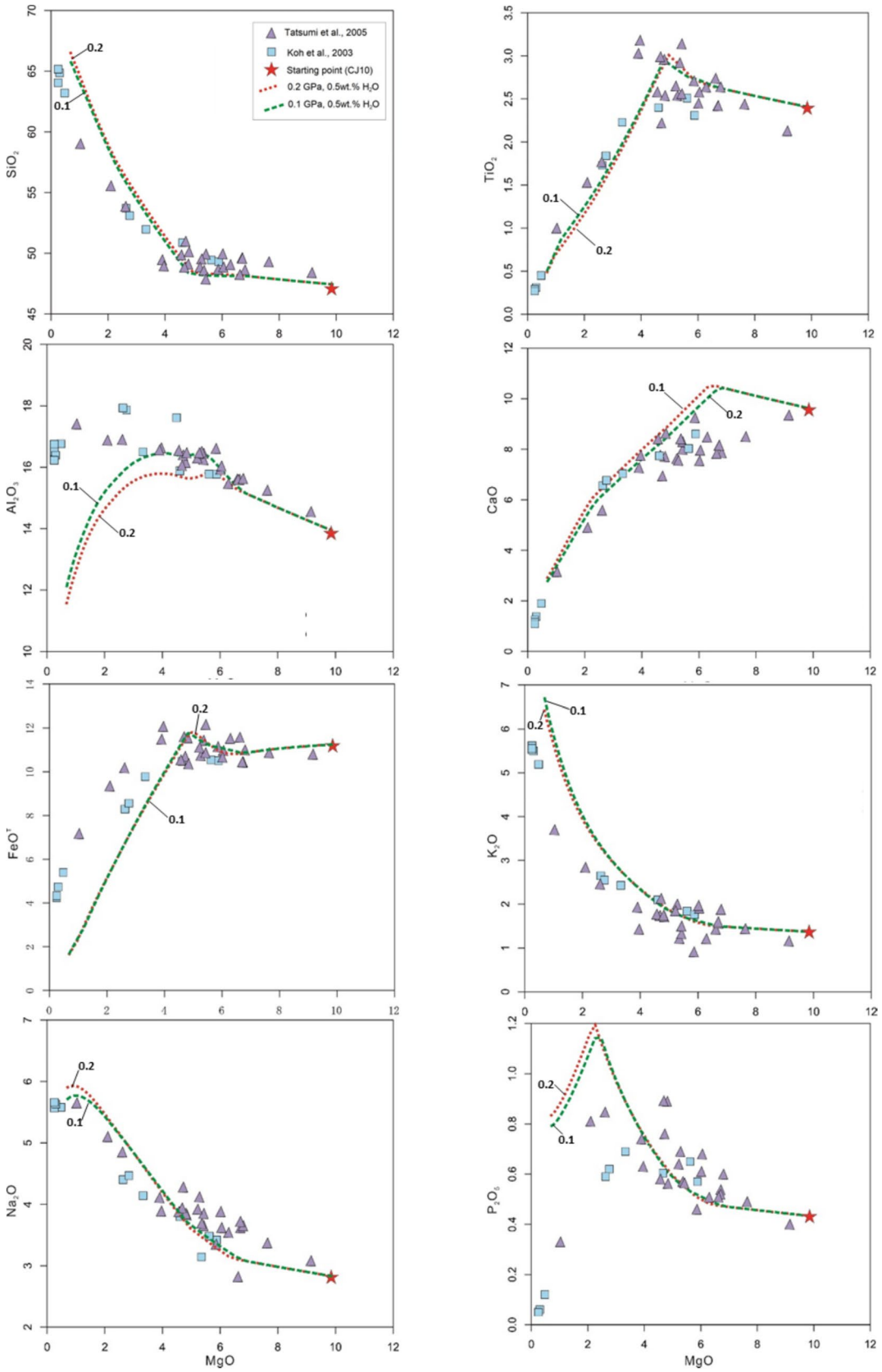

Fig. 11 (See legend on previous page.)

be the result of magma mixing instead of simple fractional crystallization. Mixtures of varying proportions between the liquid that occurs along the fractional crystallization path at 4% MgO and the starting liquid can generate the Tatsumi et al. (2005) data trend in every oxide simultaneously. If this is the correct model, there ought to be petrographic evidence in features like resorbed or rimmed phenocrysts.

11

Conclusion

This study carried out hundreds of calculations using the MELTS program, comprising rhyolite-MELTS and pMELTS, to model the fractional crystallization process of low-alumina alkaline rocks on Jeju Volcanic Island under various pressures and oxygen fugacity conditions. On the basis of the analysis of evolution paths through the TAS diagram and variation diagrams, as well as mineral compositions, the following conclusions can be drawn:

The MELTS-generated evolution paths that best match those of the natural samples from Jeju Volcanic Island feature pressures ranging from 0.2 to 0.1 GPa, an oxygen fugacity near the FMQ buffer and 0.5 wt.% H_2O.

The modeled mineral phases, such as olivine (1,270–890°C), clinopyroxene (1,170–810°C), feldspar (1,140–810°C), spinel (1,130–810°C), apatite (1,260–810°C), and rhm-oxide (970–810°C), are similar to the natural mineral assemblage of the Jeju low-alumina alkaline rocks but include spinel, magnetite and rhm-oxide phases such as ilmenite.

The model of the Jeju alkaline rocks is poorly calibrated in terms of clinopyroxene, spinel, and apatite, as demonstrated by the MgO–CaO, MgO–Al2O3 and MgO–P2O5 correlations, respectively.

Acknowledgements
This work was supported by Meteorological/Earthquake See-At Technology Development Research Grant KMI2018-02710. We would like to thank Prof. Paul D. Asimow of CALTECH for reading the paper and providing helpful comments, and the anonymous reviewers for their constructive comments and suggestions.

Author contributions
HY.L. and C.C. wrote the main manuscript text. H.L. perfomed the modeling and drew Figs. 1, 2, 3, 4, 5, 6, 7, 8, 9, 10 and 11. S-H.Y. supervised overall research. All authors discussed the results and reviewed the final manuscript.

Funding
This work was supported by Meteorological/Earthquake See-At Technology Development Research Grant KMI2018-02710.

Availability of data and materials
Not applicable.

Declarations

Competing interests
None of the authors have any financial or other interests in regard to the submitted manuscript that might be construed as a conflict of interest.

Received: 28 June 2024 Accepted: 26 September 2024
Published online: 05 October 2024

References

Asimow PD, Ghiorso MS (1998) Algorithmic modifications extending MELTS to calculate subsolidus phase relations. Am Miner 83(9–10):1127–1132
Baek S, Choi SH, Lee SG, Lee SR, Lee HM (2014) Geochemistry of anorthositic xenolith and host tholeiite basalt from Jeju Island, South Korea. Geosci J 18:125–135
Ballhaus C, Berry RF, Green DH (1990) Oxygen fugacity controls in the Earth's upper mantle. Nature 348(6300):437
Brenna M, Cronin SJ, Smith IE, Sohn YK, Németh K (2010) Mechanisms driving polymagmatic activity at a monogenetic volcano, Udo, Jeju Island, South Korea. Contrib Miner Petrol 160(6):931–950
Brenna M. 2012. Geological evolution and magmatic models for spatially and temporally variable modes of distributed volcanism, Jeju Island, Republic of Korea: a thesis presented in partial fulfillment of the requirements for the degree of Doctor of Philosophy in Earth Science at Massey University, Palmerston North, New Zealand (Doctoral dissertation, Massey University).
Brenna M, Cronin SJ, Smith IE, Maas R, Sohn YK (2012) How small-volume basaltic magmatic systems develop: a case study from the Jeju Island Volcanic Field. Korea J Petrol 53(5):985–1018
Carmichael ISE, Ghiorso MS (1990) Controls on oxidation–reduction relations in magmas. Modern Methods Igneous Petrol 24:191–212
Choi SH, Kwon ST, Mukasa SB, Sagong H (2005) Sr–Nd–Pb isotope and trace elements systematics of mantle xenoliths from Late Cenozoic alkaline lavas, South Korea. Chem Geol 211:40–64
Choi SH, Mukasa SB, Kwon ST, Andronikov AV (2006) Sr, Nd, Pb and Hf isotopic compositions of late Cenozoic alkali basalts in South Korea: Evidence for mixing between the two dominant asthenospheric mantle domains beneath East Asia. Chem Geol 232(3–4):134–151
Dingwell DB (1991) Redox viscometry of some Fe-bearing silicate melts. Am Miner 76(9–10):1560–1562
Dingwell DB, Brearley M (1988) Melt densities in the CaO-FeO-Fe2O3-SiO2 system and the compositional dependence of the partial molar volume of ferric iron in silicate melts. Geochim Cosmochim Acta 52(12):2815–2825
Gaillard F, Scaillet B, Pichavant M, Bény JM (2001) The effect of water and fO2 on the ferric–ferrous ratio of silicic melts. Chem Geol 174(1–3):255–273
Ghiorso MS, Hirschmann MM, Reiners PW, Kress VC (2002) The pMELTS: a revision of MELTS for improved calculation of phase relations and major element partitioning related to partial melting of the mantle to 3 GPa. Geochem Geophys Geosyst 3(5):1–35
Ghiorso MS, Sack RO (1995) Chemical mass transfer in magmatic processes IV. A revised and internally consistent thermodynamic model for the interpolation and extrapolation of liquid–solid equilibria in magmatic systems at elevated temperatures and pressures. Contrib Mineral Petrol 119(2–3):197–212
Gualda GA, Ghiorso MS, Lemons RV, Carley TL (2012) Rhyolite-MELTS: a modified calibration of MELTS optimized for silica-rich, fluid-bearing magmatic systems. J Petrol 53(5):875–890
Kil YW, Shin HJ, Yun SH, Koh JS, Ahn US (2008) Geochemical characteristics of mineral phases in the mantle xenoliths from Sunheul-ri, Jeju Island. J Mineral Soc Korea 21:373–382
Koh GW. 2005. Hydrogeology, groundwater occurrences and management systems of Jeju. Jeju, Korea: institute of environmental resources research, Jeju Self-Governing Province, 93.
Koh GW, Park JB, Kang BR, Kim GP, Moon DC (2013) Volcanism in Jeju Island. J Geol Soc Korea 49(2):209–230

Koh JS, Yun SH, Kang SS (2003) Petrology of the volcanic rocks in the Paekrogdam Crater area, Mt. Halla, Jeju Island. J Petrol Soc Korea 12:1–15
Lange RA, Carmichael IS (1990) Hydrous basaltic andesites associated with minette and related lavas in western Mexico. J Petrol 31(6):1225–1259
Le Bas M, Maitre RL, Streckeisen A, Zanettin B, Subcommission IUGS, on the Systematics of Igneous Rocks, (1986) A chemical classification of volcanic rocks based on the total alkali-silica diagram. J Petrol 27(3):745–750
Lee MW (1982) Petrology and geochemistry of Jeju volcanic island, Korea. Sci Report Tohoku Univ Sendai 15(2):177–256
McCammon C (2005) The paradox of mantle redox. Science 308(5723):807–808
Osborn EF (1959) Role of oxygen pressure in the crystallization and differentiation of basaltic magma. Am J Sci 257(9):609–647
Park JB (1993a) Geochemical evolution of the Cheju volcanic island: trace element chemistry of volcanic rocks from the northern part of Cheju island. J Geol Soc Korea 29:477–492
Park JB (1993b) Geochemical evolution of the Cheju volcanic island: petrography and major element chemistry for stratigraphically-controlled lavas from the northern part of Cheju Island. J Geol Soc Korea 29:39–60
Tatsumi Y, Shukuno H, Yoshikawa M, Chang Q, Sato K, Lee MW (2005) The petrology and geochemistry of volcanic rocks on Jeju Island: plume magmatism along the Asian continental margin. J Petrol 46(3):523–553
Yun SH, Koh JS, Ahn JY (1998) A study on the spinel-lherzolite xenoliths in the alkali basalt from eastern Cheju Island, Korea. J Petrol Soc Korea 31:447–458

Publisher's Note